AAPS PharmSciTech, Vol. 18, No. 1, January 2017 (© 2016)
DOI: 10.1208/s12249-016-0497-z

Research Article

Characterization and *In Vitro* Evaluation of the Complexes of Posaconazole with β- and 2,6-di-*O*-methyl-β-cyclodextrin

Peixiao Tang,[1] Lei Wang,[2] Xiaoli Ma,[1] Kailin Xu,[1] Xinnuo Xiong,[1] Xiaoxiang Liao,[1] and Hui Li[1,3]

Received 16 November 2015; accepted 1 February 2016; published online 16 February 2016

Abstract. Posaconazole is a triazole antifungal drug that with extremely poor aqueous solubility. Up to now, this drug can be administered via intravenous injection and oral suspension. However, its oral bioavailability is greatly limited by the dissolution rate of the drug. This study aimed to improve water solubility and dissolution of posaconazole through characterizing the inclusion complexes of posaconazole with β-cyclodextrin (β-CD) and 2,6-di-*O*-methyl-β-cyclodextrin (DM-β-CD). Phase solubility studies were performed to calculate the stability constants in solution. The results of FT-IR, PXRD, ^{1}H and ROESY 2D NMR, and DSC all verified the formation of the complexes in solid state. The complexes showed remarkably improved water solubility and dissolution rate than pure posaconazole. Especially, the aqueous solubility of the DM-β-CD complex is nine times higher than that of the β-CD complex. Preliminary *in vitro* antifungal susceptibility tests showed that the two inclusion complexes maintained high antifungal activities. These results indicated that the DM-β-CD complexes have great potential for application in the delivery of poorly water-soluble antifungal agents, such as posaconazole.

KEY WORDS: characterization; cyclodextrin; inclusion complex; *in vitro* antifungal testing; posaconazole.

INTRODUCTION

Posaconazole (POS, Fig. 1a), a second-generation triazole antifungal agent, is the latest itraconazole derivative that can be administered via intravenous injection and oral suspension. POS can fight against many clinically important yeasts and fungus (1,2), including *Candida* sp., *Aspergillus* sp., *Fusarium* sp., zygomycetes, and other filamentous fungi (3,4). Based on its efficient and broad-spectrum antifungal performance, POS was approved for use in the United States and the European Union for the treatment of refractory invasive fungal infections and oropharyngeal candidiasis in immunocompromised patients, as well as prophylaxis of invasive *Aspergillus* and *Candida* infections in immunocompromised patients. Especially, POS has remarkable curative effect on infections refractory to itraconazole, fluconazole, or both (5,6).

Although POS has numerous pharmacological effects, its poor water solubility greatly limits its clinical application. Previous reports indicated that the bioavailability of POS in oral suspension under fasting conditions is low because of its poor solubility (7). However, the concomitant administration of a high-fat meal or a liquid nutritional supplement with POS oral suspension can enhance POS bioavailability in patients (8,9). This enhancement presumably results from the increased solubility (7). These reports demonstrated that better water solubility and higher dissolution rate of POS will be beneficial to improve the bioavailability of its oral preparation. Previous published patents reported novel POS injection methods using modified cyclodextrin (CD) as a solubilizer and dissolving in mixed solvent comprising organic solvent and water (10,11). However, the basic inclusion interactions and physicochemical properties of the CD/POS binary system still need further exploration.

The cyclodextrin (CD) inclusion complex is highly efficient in enhancing water solubility and dissolution of hydrophobic drugs (12–14). CDs, which are macrocyclic oligosaccharides derived from starch, are composed of glucose units linked by α-1,4-glycosidic bonds in a cyclic manner (15). In general, CDs possess a truncated conical shape and feature structures with a hydrophobic cavity, hydrophilic ends, and an external portion. CDs exhibit an important function in the field of supramolecular chemistry, as many types of guest molecules can be accommodated into their cavities (16,17). In addition, CDs have been widely used as encapsulating agents to improve the solubility, dissolution rate, stability, and bioavailability of drug molecules (18,19). Especially, in the cyclodextrins, 2,6-di-*O*-methyl-β-cyclodextrin (DM-β-CD) shows two obvious advantages than the others: the higher water solubility which can get the better solubilization effect,

Electronic supplementary material The online version of this article (doi:10.1208/s12249-016-0497-z) contains supplementary material, which is available to authorized users.

[1] College of Chemical Engineering, Sichuan University, Chengdu, 610065, China.
[2] Sichuan Guang'an Food and Drug Administration, Guang'an, 638000, China.
[3] To whom correspondence should be addressed. (e-mail: lihuilab@sina.com)

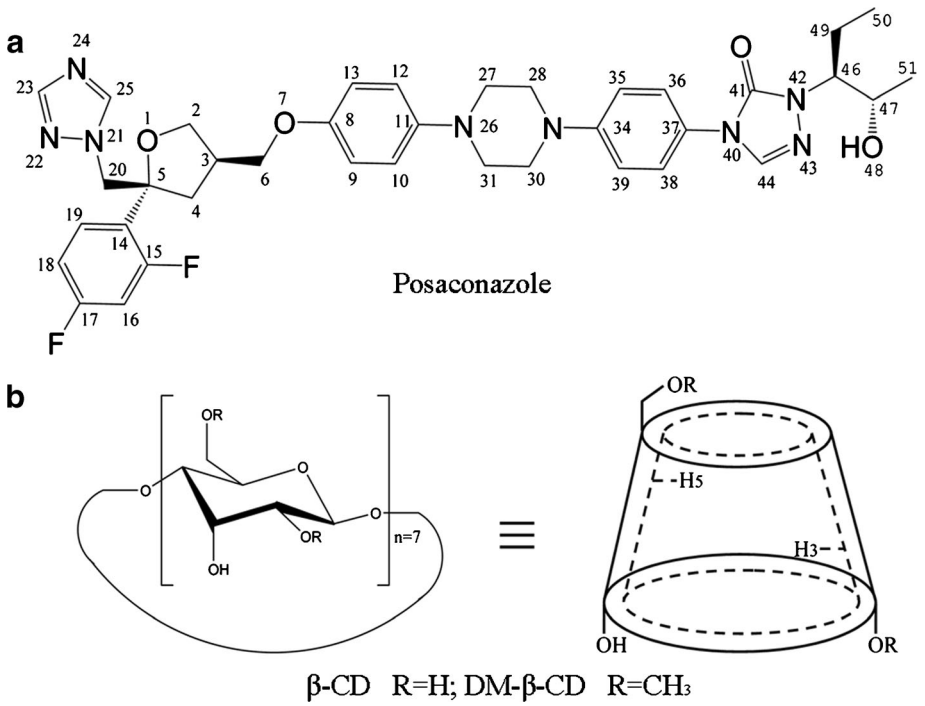

Fig. 1. Structures of posaconazole (**a**), and β-cyclodextrin and 2,6-di-*O*-methyl-β-cyclodextrin (**b**)

and moderate substitution degree which lead to small space steric hindrance.

In the present study, we aimed to prepare the solid water-soluble complexes of CDs and posaconazole for *in vitro* antifungal research, which provide theoretical basis for the study of the novel POS solid dosage form. Thus, the complexes of POS with β-cyclodextrin (β-CD) and 2,6-di-*O*-methyl-β-cyclodextrin (Fig. 1b) were prepared and investigated. Drug/CD interactions in solution were studied by phase solubility study. The solid complexes were characterized by Fourier transform infrared spectrometry (FT-IR), powder X-ray diffraction (PXRD), ^{1}H and rotating-frame Overhauser effect spectroscopy (ROESY) nuclear magnetic resonance spectroscopy (NMR), differential scanning calorimetry (DSC), and scanning electron microscopy (SEM), aiming to confirm the formation of the inclusion complexes. Molecular modeling was performed to verify the geometric configuration of the complexes from experiment results. The solubility and dissolution rates of the complexes were investigated. Finally, the antifungal activities of the complexes were evaluated to detect whether antifungal bioactivity is retained.

MATERIAL AND METHODS

Chemicals and Reagents

POS (formula weight (FW) = 700.78, purity ≥ 98%) was purchased from Schering-Plough Research Institute (Kenilworth, NJ, USA). β-CD (FW = 1134.98, purity ≥ 98%) and DM-β-CD (DS = 2.0, FW = 1331.39, purity ≥ 98%) were purchased from Sigma-Aldrich Chemical Company (Shanghai, China); both the CDs were used without further purification. All other regents and solvents used were of analytical grade and were purchased from Ke-Long Chemical Reagent Factory (Chengdu, China). Triple-distilled water was used throughout the experiment.

Synthesis of Inclusion Complexes

POS (20 mmol) completely dissolved in 1:4 (*v*/*v*) acetone/methanol was added dropwise to aqueous solutions of β-CD and DM-β-CD. The mixed solutions were stirred at a controlled temperature of 40 ± 1°C for 12 h and then heated to 65°C to remove the organic solvents. The obtained solutions were filtered, gradually cooled to room temperature, and refrigerated at −20°C. The completely frozen solutions were dried in a laboratory vacuum freeze dryer. The resulting solid complexes were passed through a 60-mesh sieve and stored in sealed glass vial.

Phase Solubility Studies

Phase solubility studies were carried out based on the methods described by Higuchi and Connors (20). Excess amount of POS (30 mg) was added to aqueous solutions of β-CD and DM-β-CD with various concentrations (0 to 15.00 mM for β-CD and 0 to 35.00 mM for DM-β-CD). After 15 min of ultrasonic irradiation, the mixtures were left to stand for 10 days at 15, 25, and 37°C. When equilibrium was achieved, each solution was filtered through a Millipore membrane (0.45 μm), properly diluted, and detected at 263 nm by a TU-1901 ultraviolet-visible (UV-Vis) spectrophotometer (Persee, China) to calculate the concentration of POS according to the standard curve: $Y = 0.0521X + 0.1355$, $R^2 = 0.9998$. All experiments were performed in triplicate.

Characterization of the Complexes

The FT-IR spectra of POS, β-CD, DM-β-CD, their physical mixtures, and inclusion complexes were obtained on a

Nicolet 6700 FT-IR spectrometer (Thermo Fisher Scientific, USA) using the KBr disk technique. Samples were prepared as KBr disk with 1 mg of sample in 100 mg of KBr. Scanning was performed from 4000 to 400 cm^{-1}.

PXRD patterns were obtained from a PANalytical X'Pert PRO diffractometer using Cu Kα1 radiation ($\lambda = 1.54056$ Å, generator setting: 40 kV, 40 mA). Scanning was performed with a step size of 0.01313° (2θ) and a counting time of 30 ms/step in a diffraction angle (2θ) ranging from 5 to 50°.

DSC was performed at a heating rate of 10°C/min ranging from 30 to 350°C in a dynamic nitrogen atmosphere. The samples were sealed in closed alumina crucibles before analysis by a differential scanning calorimeter (TA, USA).

^{1}H-NMR spectra of the samples were recorded on a Bruker Avance 400 spectrometer (Germany) at 25°C using a 5-mm probe and a simple pulse-acquire sequence. Experiments were run with an FID resolution of 0.13 Hz/point; spectral width of 8223 Hz, acquisition time of 3.98 s, 16 scans, and relaxation delay of 1 s. Chemical shifts were reported in parts per million (ppm). Two-dimensional (2D) ROESY experiments were recorded on a Bruker Avance 600 spectrometer (Germany) at 25°C with a mixing time of 300 ms. D_2O was used to dissolve the samples.

The SEM images of the samples were collected by a JSM-7500F scanning electron microscope (JEOL). Prior to analysis, all samples were coated with gold to confer electrical conductivity.

Molecular Modeling

Molecular modeling was performed using the Lamarckian genetic algorithm in Auto Dock 4.0 software (Accelrys Co., Ltd., USA). The structures of β-CD and DM-β-CD molecules were obtained from the Cambridge Structural Database (Ref. code: BCDEX03 for β-CD; Ref. Code: BOYFOK03 for DM-β-CD). The POS molecule was drawn and optimized with Materials Studio 4.2 software (Accelrys Co., Ltd., USA). ΔE of the minimum energy mode was calculated according to Eq. 1: $\Delta E = E_{complex} - (E_{host} + E_{guest})$, where $E_{complex}$, E_{host}, and E_{guest} are the calculated energies of inclusion complexes, CD, and POS molecules, respectively.

Solubilization Study

Water solubility of both complexes was evaluated by the preparation of saturated solutions. Excess amounts of pure POS and the two complexes were added to 2 mL of water, and the suspensions were stirred for 48 h at 25 ± 1°C. The obtained solutions were then filtered through a Millipore membrane (0.45 μm) to remove the insoluble substances. The POS concentrations were then calculated based on the absorbance of the filtrate detected by UV at 263 nm.

In Vitro Dissolution Studies

Dissolution studies were performed using an intelligent supply ZRC-8D Dissolution Tester (Tongdechuangye, China) at 50 rpm and 37 ± 0.5°C. The conditions were maintained throughout the period of dissolution studies. POS (30 mg) and known amounts of the physical mixtures and the complexes equivalent to 30 mg of POS were passed through an 80-mesh sieve and separately added to 1000 mL of triple-distilled water. The samples (5 mL) were withdrawn using syringes at pre-specified time intervals. Each sample was then filtered through a hydrophilic membrane filter (0.45 μm) and analyzed by a UV spectrophotometer at 263 nm.

In Vitro Antifungal Susceptibility Testing

Organisms

Several kinds of common pathogenic fungi were chosen as the test organisms. Clinical isolates (738 *Candida albicans*, 409 *Aspergillus fumigates*, 145 *Aspergillus niger*, and 25 *Penicillium* spp.) obtained from different medical centers in North America, South America, Europe, and Asia were tested. The isolates were all recent clinical isolates, and the majority was from blood or normally sterile body fluids. The isolates were identified by standard methods (21) and stored as spore suspensions in sterile triple-distilled water until use. Before being tested, each isolate was subcultured at least twice on potato dextrose agar (Remel, Lenexa, KS, USA) to ensure viability and purity.

Antifungal Susceptibility Studies

The hole-punch method was initially applied to investigate the antifungal activities of the inclusion complexes. Subsequently, antifungal susceptibility testing was performed by microdilution according to the guidelines of the National Committee for Clinical Laboratory Standards (NCCLS) document M27-A (22). Stock solutions of POS and CD-POS complexes were prepared in polyethylene glycol. Stock solutions were diluted with RPMI 1640 medium (with glutamine) supplemented with glucose (2%, *w*/*v*), buffered to pH 7.0 with 0.165 M morpholinepropanesulfonic acid buffer (Sigma), and dispensed into 96-well micro dilution trays. Trays containing a 0.1-mL aliquot of the appropriate drug solution in each well were subjected to quality control, sealed, and stored at −70°C until use. The final concentrations of the drugs in the wells ranged from 7×10^{-3} to 16 μg/mL, with each concentration has six parallel groups. The stock conidial suspension (10^6 spores/mL) was diluted to a final inoculum concentration of 1.0×10^4 to 5.0×10^4 CFU mL^{-1} and dispensed into microdilution wells. Drug-free and yeast-free controls were included.

The inoculated microdilution trays were incubated at 28°C, and minimal inhibitory concentration (MIC) endpoints were read after 48 h of incubation. The MICs were read as the lowest concentration at which a prominent decrease (approximately 50%) in turbidity relative to the turbidity of the growth control was observed (22).

Quality Control and Statistical Analysis

Quality control was performed by testing the following strains (22,23): *Aspergillus flavus* ATCC 204304, *Candida parapsilosis* ATCC 22019, and *Candida krusei* ATCC 6258. All results were within the recommended limits of the NCCLS (22) or other published limits if NCCLS recommended limits were unavailable (23). Statistical analyses used one-way analysis of variance (ANOVA) test with Duncan's multiple range test. $P < 0.05$ was considered to indicate a statistically significant difference.

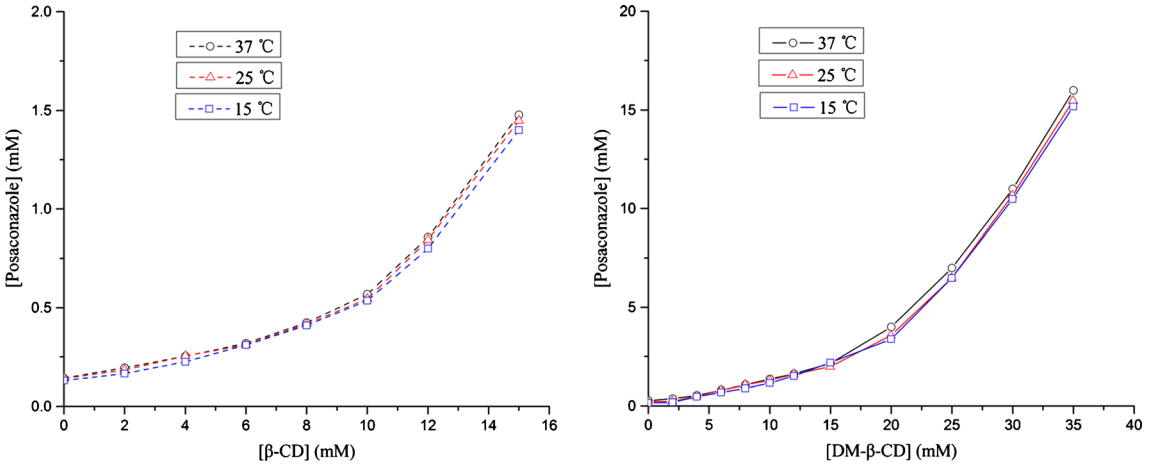

Fig. 2. Phase solubility diagrams of POS in the presence of β-CD and DM-β-CD at 15, 25, and 37°C

RESULTS AND DISCUSSION

Phase Solubility Studies

Phase solubility study provides not only the solubilizing ability but also the apparent stability constant of the complex by analyzing the phase solubility diagrams (20). The phase solubility curve of POS in the presence of CDs at 15, 25, and 37°C are shown in Fig. 2. The curves demonstrated a curvilinear dependence of POS solubility on CD concentration. Based on a previous study by Higuchi and Connors, all curves can be classified as A_p type (20). These results demonstrated the formation of 1:1 complex at lower CD concentration and 1:*n* complex at higher CD concentration, which was similar to the inclusion process of previous complexes of CDs with azole antifungal agents (24,25). Thus, the upward curvatures were quantitatively analyzed according to the optimization technique to obtain the stability constants of higher order complex ($K_{1:n}$) (26).

$$[S]_t = S_0 + K_{1:1} \cdot S_0 \cdot [\mathrm{CD}] + K_{1:1} \cdot K_{1:2} \cdot S_0 \cdot [\mathrm{CD}]^2 + \cdots + K_{1:1} \cdot K_{1:2} \cdots K_{1:n} \cdot S_0 \cdot [\mathrm{CD}]n \quad (1)$$

$$[\mathrm{CD}]_t = [\mathrm{CD}] + K_{1:1} \cdot S_0 \cdot [\mathrm{CD}] + 2 \cdot K_{1:1} \cdot K_{1:2} \cdot S_0 \cdot [\mathrm{CD}]2 + \ldots + n \cdot K_{1:1} \cdot K_{1:2} \ldots K_{1:n} \cdot S_0 \cdot [\mathrm{CD}]n \quad (2)$$

where $K_{1:1}$, $K_{1:2}$,…$K_{1:n}$ are the stability constants of the complexes with stoichiometry of 1:1,1:2,…1:*n* (drug:CD), S_0 is the solubility of POS in the absence of CD, $[S]_t$ is the total concentration of POS, and [CD] and $[CD]_t$ represent the free and total concentrations of CDs, respectively. By setting $[CD]_t = [CD]$ as a first approximation, Eq. (1) was analyzed by a nonlinear least-squares optimization approach to obtain the apparent stability constant. The [CD] value was then calculated from Eq. (2) using the above apparent stability constant. This procedure was repeated until the stability constant converged at a constant value. The results of this procedure and the approach of Higuchi and Kristiansen indicated that the quadratic model, which assumes second-order complexation, was applicable to the phase solubility data obtained in our study. These results demonstrated the formation of 1:2 complexes at higher CD concentration.

The apparent stability constants and the thermodynamic parameters obtained are displayed in Table I. The constant values were in the range of 50–2000 M^{-1}, implying its potential for practical applications (27,28). The stability constants of the DM-β-CD complexes were distinctly higher than those of the parent β-CD. The enhanced performance of the derivatives is attributed to the presence of the methyl substituent that expanded the hydrophobic region of the cavity and the increased substrate binding via a hydrophobic effect.

In addition, the intrinsic solubility of POS and the stability constants of the complexes slightly increased with the increase in temperature. The influence of temperature on the solubilization of the drug was negligible under experimental conditions.

Table I. Calculated Apparent Stability Constants of the Two Complexes at 15, 25, and 37°C Obtained from Phase Solubility Studies. ($n = 3$, Values Are the Mean ± SD of Triplicate Experiments)

	T (°C)	$K_{1:1}$ (M^{-1})	$\Delta G_{1:1}$ (kJ·mol^{-1})	$\Delta H_{1:1}$ (kJ·mol^{-1})	$\Delta S_{1:1}$ (J·mol^{-1}·K^{-1})	$K_{1:2}$ (M^{-1})	$\Delta G_{1:2}$ (kJ·mol^{-1})	$\Delta H_{1:2}$ (kJ·mol^{-1})	$\Delta S_{1:2}$ (J·mol^{-1}·K^{-1})
β-CD/POS	15	296.66 ± 4	−13.71 ± 0.3	1.24 ± 0.01	51.59 ± 0.3	935.42 ± 9	−16.60 ± 0.2	3.09 ± 0.02	67.63 ± 0.4
	25	300.28 ± 5	−14.13 ± 0.2			983.19 ± 9	−17.07 ± 0.3		
	37	307.12 ± 4	−14.67 ± 0.4			1025.44 ± 11	−17.63 ± 0.5		
DM-β-CD/ POS	15	393.25 ± 6	−14.38 ± 0.2	1.07 ± 0.01	53.37 ± 0.02	1269.53 ± 11	−17.24 ± 0.4	1.84 ± 0.04	65.78 ± 0.05
	25	398.13 ± 5	−14.83 ± 0.3			1296.27 ± 9	−17.76 ± 0.3		
	37	405.86 ± 5	−15.40 ± 0.2			1340.29 ± 12	−18.42 ± 0.3		

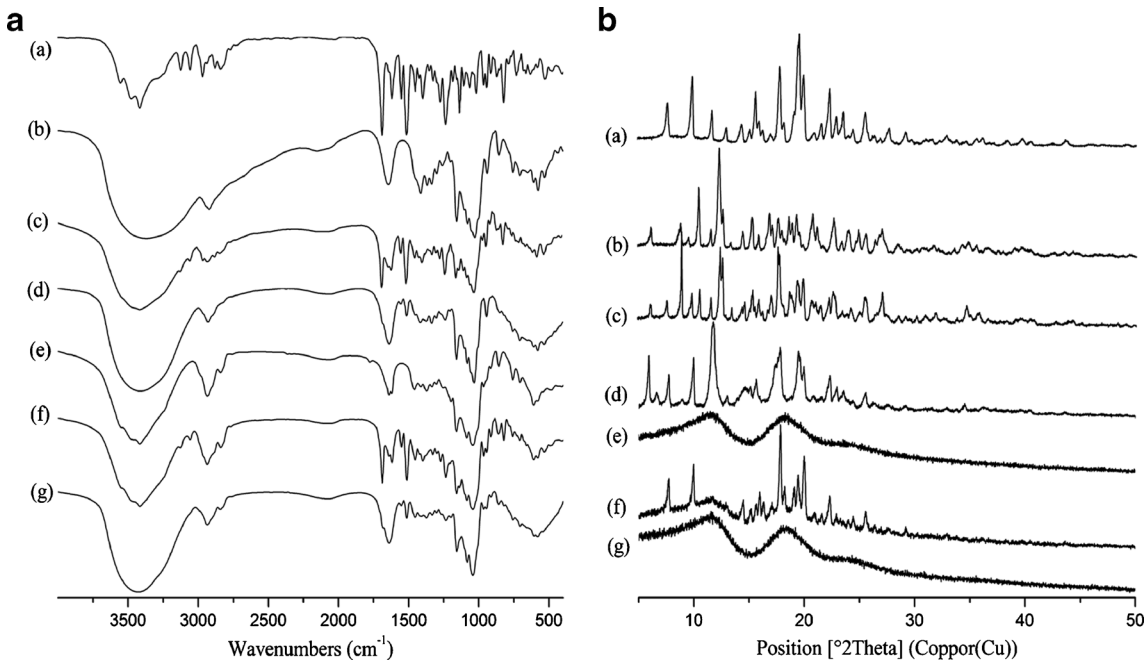

Fig. 3. FT-IR spectra (**a**) and PXRD patterns **(b)** of POS (*a*), β-CD (*b*), β-CD/POS physical mixture (*c*), β-CD–POS inclusion complex (*d*), DM-β-CD (*e*), DM-β-CD/POS physical mixture (*f*), and DM-β-CD–POS inclusion complex (*g*)

Characterization of the Inclusion Complexes

FT-IR

The FT-IR results provide evidence of the formation of β-CD–POS and DM-β-CD–POS inclusion complexes. Shifts in characteristic bands, disappearance or reduction in intensity, and appearance of new bands in the FT-IR spectra might be related to possible drug–CD interactions or amorphization of the product (29). The FT-IR spectra of pure POS, β-CD, DM-β-CD, drug/CD physical mixtures, and the inclusion complexes are illustrated in Fig. 3. The spectrograph of POS [Fig. 3a (a)] shows high-intensity absorption peaks at 3121, 2965, 1686, 1617, and 1423 cm^{-1} corresponding to the stretching vibrations of OH, CH_2, C = O, C = N, and C–N, respectively. The spectra of the physical mixtures [Fig. 3a (c, f)] corresponded to the simple superposition of the spectra of individual components. Characteristic absorption peaks of POS were noticeable, indicating that POS remained in the physical mixture without any interactions with CDs. However, the spectra of the inclusion complexes [Fig. 3a (d, g)] exhibited a reduced intensity and a shift in bands. The absorption band at 1686 cm^{-1} was significantly reduced, indicating that C = O may have had a strong interaction with the hydrogen-bond donor of CD. The absorption peaks of C = N and C–N shifted to low wavenumbers in the two complexes, indicating that the groups may be embedded into the CD cavities. These findings demonstrated the formation of the two inclusion complexes with the C = O, C = N, and C–N groups possibly embedded into the CD cavity.

PXRD

Further evidence of the formation of the two inclusion complexes were obtained from the PXRD results. When a true inclusion complex is formed, the diffraction pattern of the complex is distinct from that of the superposition of the free components (30). Figure 3b illustrates the PXRD patterns of the free components and the complexes. The patterns of POS [Fig. 3b (a)] and β-CD [Fig. 3b (b)] showed several sharp and intense peaks at different diffraction angles, suggesting that the POS and β-CD existed as crystals. The pattern of DM-β-CD [Fig. 3b (e)] showed two broad peaks in the 10–25° (2θ) range, indicating the amorphous character of this compound. The patterns of the physical

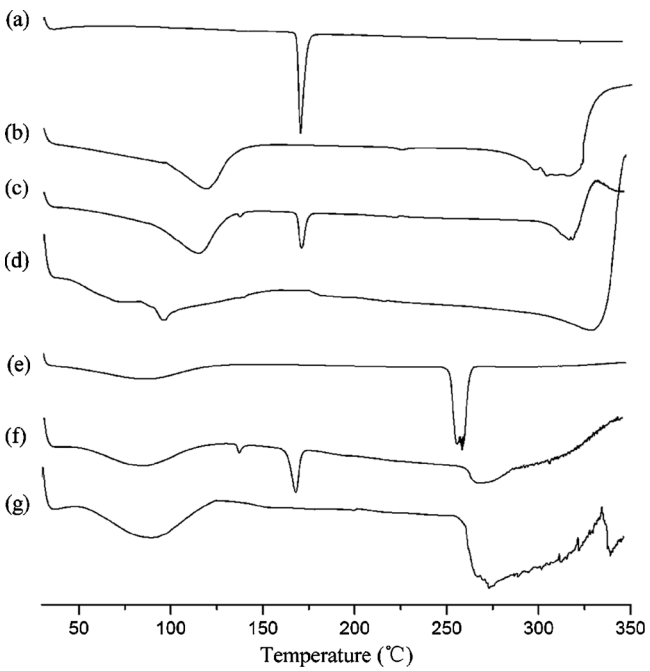

Fig. 4. DSC curves of POS (*a*), β-CD (*b*), β-CD/POS physical mixture (*c*), β-CD–POS inclusion complex (*d*), DM-β-CD (*e*), DM-β-CD/POS physical mixture (*f*), and DM-β-CD–POS inclusion complex (*g*)

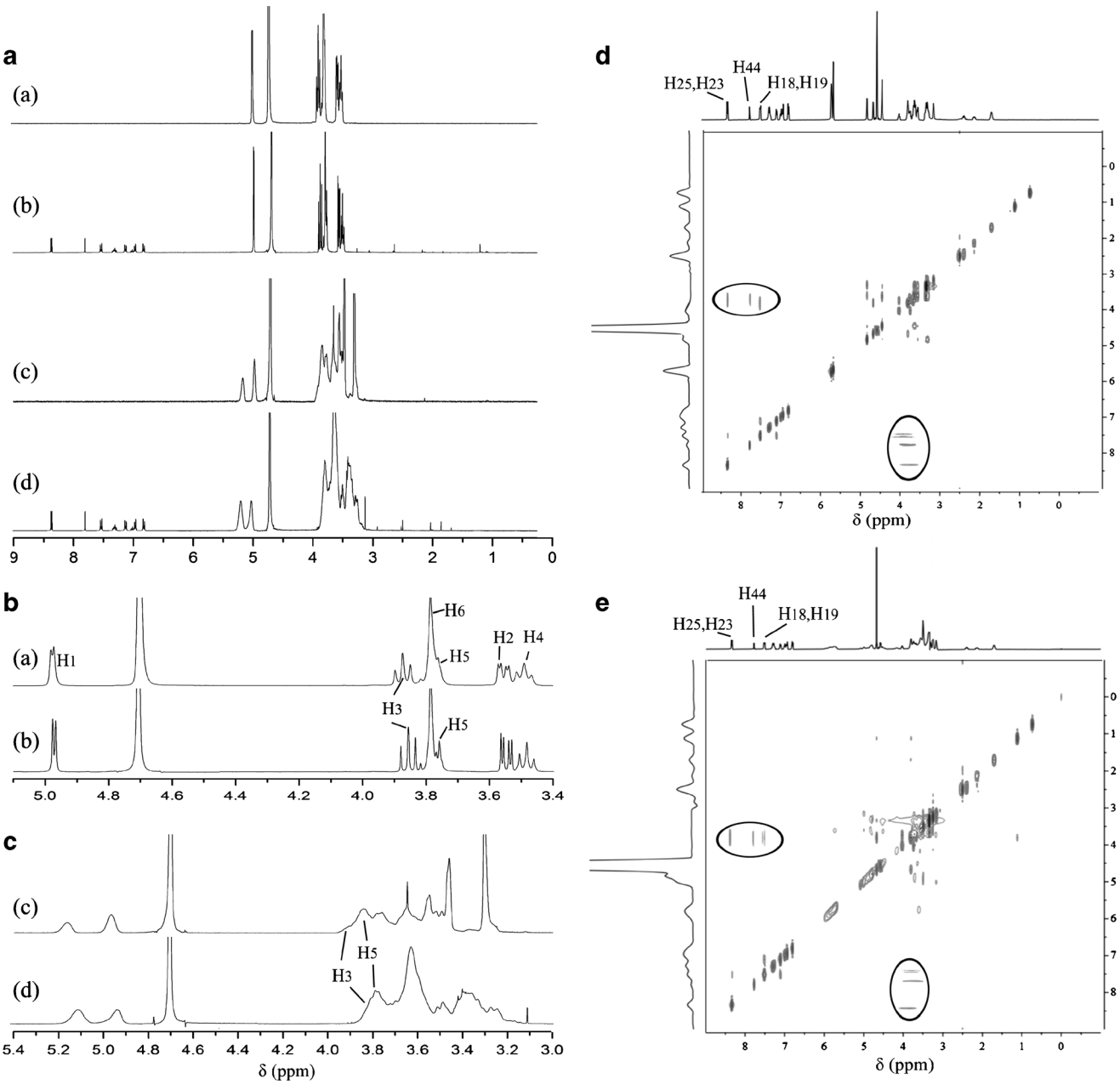

Fig. 5. **a** ^{1}H-NMR spectra of β-CD (*a*), β-CD–POS inclusion complex (*b*), DM-β-CD (*c*), and DM-β-CD–POS inclusion complex (*d*) in D_2O; **b** Partial enlarged drawings of the superimpose NMR spectra of β-CD (*a*) and β-CD–POS inclusion complex (*b*); **c** Partial enlarged drawings of the superimpose NMR spectra of DM-β-CD (*c*) and DM-β-CD–POS inclusion complex (*d*); **d** 2D ROSEY patterns of the β-CD–POS inclusion complex; and **e** DM-β-CD–POS inclusion complex in D_2O

mixtures of POS and the two CDs were the superposition of the patterns of individual components. However, the PXRD pattern of β-CD–POS complex [Fig. 3b(d)] showed reduction or disappearance of the characteristic diffraction peaks of POS, as well as emergence of new peaks, indicating the formation of the β-CD–POS inclusion complex. The pattern of the DM-β-CD–POS complex [Fig. 3b (g)] exhibited broad bands in which the characteristic peaks of POS completely disappeared. This phenomenon confirmed that the DM-β-CD–POS complex was formed without free POS. This modification of crystals could be taken as evidence of the formation of the inclusion complexes.

DSC

The melting, boiling, or sublimating points of a guest molecule can generally shift to different temperatures or disappear when it is embedded into CD cavities (31). The DSC curves of POS, physical mixtures, and the inclusion complexes are shown in Fig. 4. A strong endothermic peak appeared at 171°C in the thermogram of free POS, corresponding to its melting point. Endothermic peaks were observed from 75 to 125°C in the CD curves, indicating water loss. The physical mixtures showed a superposition of the endothermic peaks of the free components, which indicated that no interaction

existed between the host and guest molecules in the physical mixture. However, in the DSC curves of inclusion complexes [Fig. 4d, g], the endothermic peak at 171°C disappeared entirely, indicating the absence of free POS from the complexes. These phenomena possibly resulted from the POS molecule, which was embedded into cavities of the CDs to form stable complexes.

^{1}H and ROSEY 2D NMR

NMR results exhibited the strongest evidence of inclusion complex formation. As a powerful tool for the study of CD inclusion complexes, NMR spectroscopy has been used to establish inclusion modes. When a guest molecule is embedded into the CD cavity to form a complex, the chemical shifts of the hydrogen atoms inside the CD cavity (H-3 and H-5) become shielded and generally exhibit a noticeable upfield shift; however, the hydrogen atoms outside the cavity (H-1, H-2, and H-4) experience only a marginal shift upon complexation (32,33).

To investigate the possible inclusion mode of the two CD-POS complexes, the ^{1}H-NMR spectra of pure CDs, and the inclusion complexes in D_2O were studied and presented in Fig. 5a. The partial enlarged drawings were illustrated in Fig. 5b, c. Chemical shifts and changes in the complexes are listed in Table II. In the comparisons of protons chemical shifts in D_2O, distinct chemical shift variations in the H-3 and H-5 protons were observed with $\Delta\delta$ values of −0.026 and −0.012 ppm, respectively, for β-CD, and −0.065 and −0.032 ppm, respectively, for DM-β-CD. The shifts of the above protons may result from the increase in the electron cloud over these protons after a portion of the POS entered the CD cavities to form the complexes. The other protons (H-1, H-2, and H-4) located outside the cavity present subtle differences compared to the free CDs. These phenomena indicate that POS may have been inserted into the CD cavities.

The ROESY spectroscopy provides important information about the spatial proximity between host and guest atoms by observation of intermolecular dipolar cross-correlations (34). Two protons that are closer than 4 Å in space can produce a nuclear Overhauser effect (NOE) cross-correlation in ROESY (34). To gain additional conformational information, the 2D ROESY spectra of the β-CD–POS (Fig. 5d) and DM-β-CD–POS (Fig. 5e) complexes in D_2O were obtained. Key correlations were observed between the H-18, H-19, H-23, H-25, and H-44 protons of POS and the H-5 and H-3 protons of the CDs. These results indicate that the triazole and triazolone rings of POS were embedded into the CDs cavities to form the inclusion complexes.

The results of ^{1}H and ROESY 2D NMR studies confirmed the formation of the two inclusion complexes, in which the triazole and triazolone rings of POS were embedded into the CDs cavities. These findings corroborated the results of FT-IR, PXRD, and DSC.

SEM

SEM is a qualitative method used to investigate the surface morphology of drugs, CDs, and other materials (35,36). Figure S1 displays the SEM images of all the samples. Pure POS exists in a crystalline state with a flaky morphology in different sizes. β-CD shows an irregular shape, whereas DM-β-CD presents a spherical shape accompanied with some fragments. The physical mixtures clearly presented the characteristics of both components, with the POS mixed with CDs or adhered to their surface. However, the two inclusion complexes exhibit irregular morphologies, which differed from the free components and the physical mixtures. The original morphology of POS and CDs disappeared, suggesting that new mineral phases formed. The above changes may result from the formation of the two inclusion complexes. These findings can be assumed as forceful support to the PXRD studies.

Taken together, the above characterization results confirmed the formation of the β-CD–POS and DM-β-CD–POS complexes, in which the triazole and triazolone rings of POS were embedded into the CD cavities.

Molecular Modeling

Molecular modeling, a theoretical study of the interactions between the host and guest molecules, was performed to find the most possible configuration of the inclusion complexes and to verify the above experimental results.

Table II. Variation in the ^{1}H NMR Chemical Shifts (δ/ppm) of β-CD and DM-β-CD Protons in Free and Complex States Determined in D_2O at 25°C

Substance	Proton	Free (δ)	Complex (δ)	$\Delta\delta$
β-CD	H-1	4.966	4.960	−0.006
	H-2	3.564	3.557	−0.007
	H-3	3.877	3.851	−0.026
	H-4	3.485	3.481	−0.004
	H-5	3.758	3.746	−0.012
	H-6	3.797	3.796	−0.001
DM-β-CD	H-1	4.967	4.959	−0.008
	H-2	3.637	3.632	−0.005
	H-3	3.906	3.841	−0.065
	H-4	3.528	3.519	−0.009
	H-5	3.824	3.792	−0.032
	H-6	3.788	3.780	−0.008
	OMe-2	3.494	3.487	−0.007
	OMe-6	3.250	3.248	−0.002

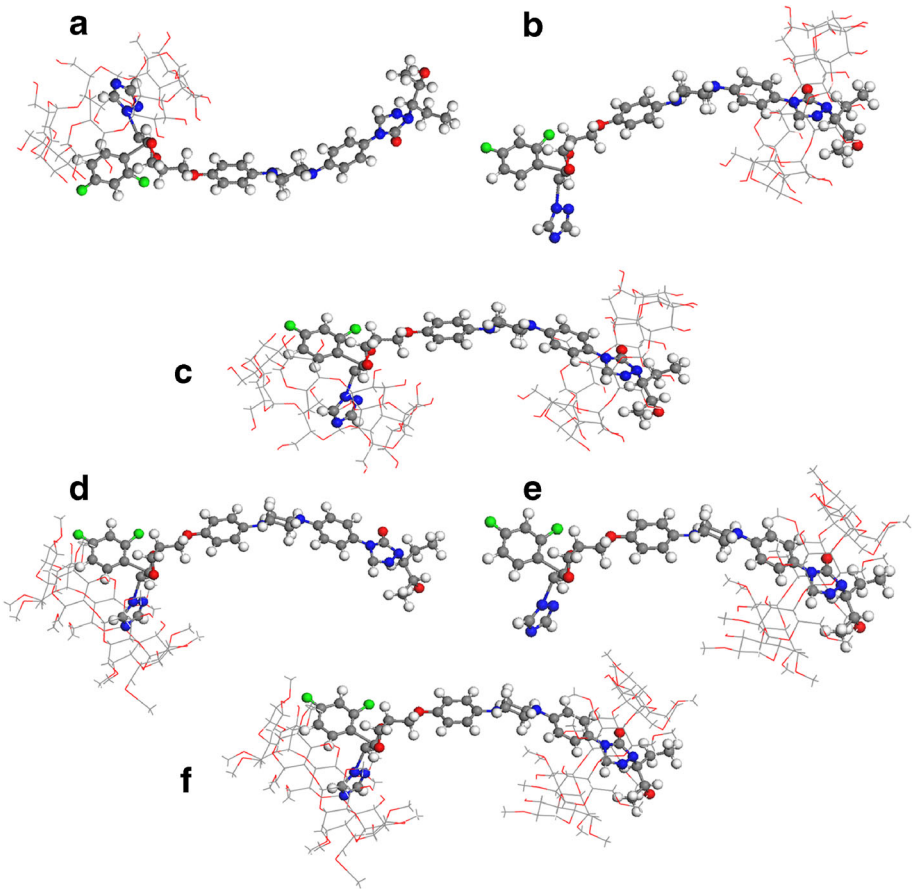

Fig. 6. Models of the inclusion complexes of POS with β-CD and DM-β-CD with different configurations as obtained from docking calculations. Triazolemoiety (*a*), triazolonemoiety (*b*), and two sides of β-CD–POS complex (*c*). Triazolemoiety (*d*), triazolonemoiety (*e*), and two sides of DM-β-CD–POS complex (*f*)

The optimized geometry docking results are illustrated in Fig. 6. The ΔE values of the complexes were calculated for the minimum energy mode according to Eq. (1) based on the data of E_{host}, E_{guest}, and $E_{complex}$, and the results are displayed in Table III. For the 1:1 stoichiometry, the ΔE values were −5.32 (model a) and −13.84 kcal/mol (model b) for β-CD–POS complexes, and −10.86 (model e) and −12.47 kcal/mol (model f) for DM-β-CD–POS complexes. For the 2:1 stoichiometry, the ΔE values were −31.63 (model c) and −38.06 kcal/mol (model f) for β-CD–POS and DM-β-CD–POS, respectively. These results indicated that the 1:2 drug–CD complexes were the most predominant configuration, in which the triazole and triazolone rings of POS were inserted into the CD cavities due to hydrophobic interactions and hydrogen bonds. In addition, the lower interaction energy value of DM-β-CD–POS complex indicates that the DM-β-CD complex is more stable than the β-CD complex. This high stability may also be attributed to the presence of the methyl substituent that increased substrate binding via a hydrophobic effect. These findings were consistent with the results of phase solubility studies, FT-IR, and NMR.

Solubilization Study

The results of solubilization studies indicated that the water solubility of POS significantly increased from 0.12 (RSD = 0.82%) to 1.15 mg/mL (RSD = 0.71%, $P < 0.001$) and 10.87 mg/mL (RSD = 0.74%, $P < 0.001$) after complexation with β-CD and DM-β-CD, respectively, which indicates 9.6 and 90.5 times enhancement. This significant enhancement

Table III. Interaction Energy of β-CD/POS and DM-β-CD/POS Complexes

Models	CD:POS	$E_{complex}$ (kcal/mol)	$E_{host} + E_{guest}$ (kcal/mol)	ΔE (kcal/mol)
β-CD/POS (triazolemoiety)	1:1 (a)	−2734.13	−2729.45	−5.32
β-CD/POS (triazolonemoiety)	1:1 (b)	−2743.29	−2729.45	−13.84
β-CD/POS (two sides)	2:1 (c)	−4496.84	−4465.21	−31.63
DM-β-CD/POS (triazolemoiety)	1:1 (d)	−2914.08	−2903.22	−10.86
DM-β-CD/POS (triazolonemoiety)	1:1 (e)	−2915.69	−2903.22	−12.47
DM-β-CD/POS (two sides)	2:1 (f)	−4850.81	−4812.75	−38.06

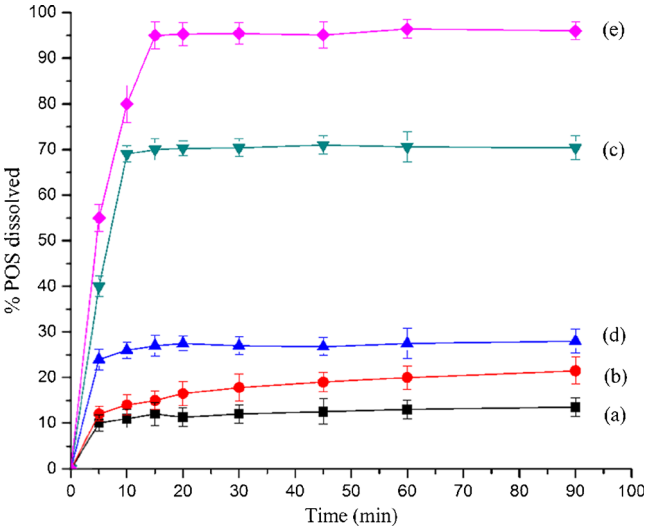

Fig. 7. Dissolution curves of POS (■), β-CD/POS physical mixture (●), β-CD–POS inclusion complex (▼), DM-β-CD/POS physical mixture (▲), and DM-β-CD–POS inclusion complex (♦) in water

confirmed that CDs increased the water solubility of POS by forming hydrophilic inclusion complexes, which was favorable for the medical utilization of POS. In addition, the DM-β-CD–POS complex showed about nine times higher solubility than the β-CD–POS complex, such phenomenon was possibly because DM-β-CD is more efficient in solubilization than β-CD.

In Vitro Dissolution Rate

The influence of CDs on the dissolution of POS was investigated through a comparison of the dissolution profiles of POS before and after complexation with β-CD and DM-β-CD (Fig. 7). Pure POS showed approximately 10% dissolution after 90 min because of its poor water solubility. The physical mixtures of POS with β-CD or DM-β-CD exhibited 15 and 19% ($P < 0.05$) dissolution, respectively, which indicated the difficulty of enhancing the drug dissolution rate via simple mixing with CDs. By contrast, the inclusion complexes showed significantly better dissolution rates than free POS and the physical mixtures. The complexes exhibited about 40 and 55%

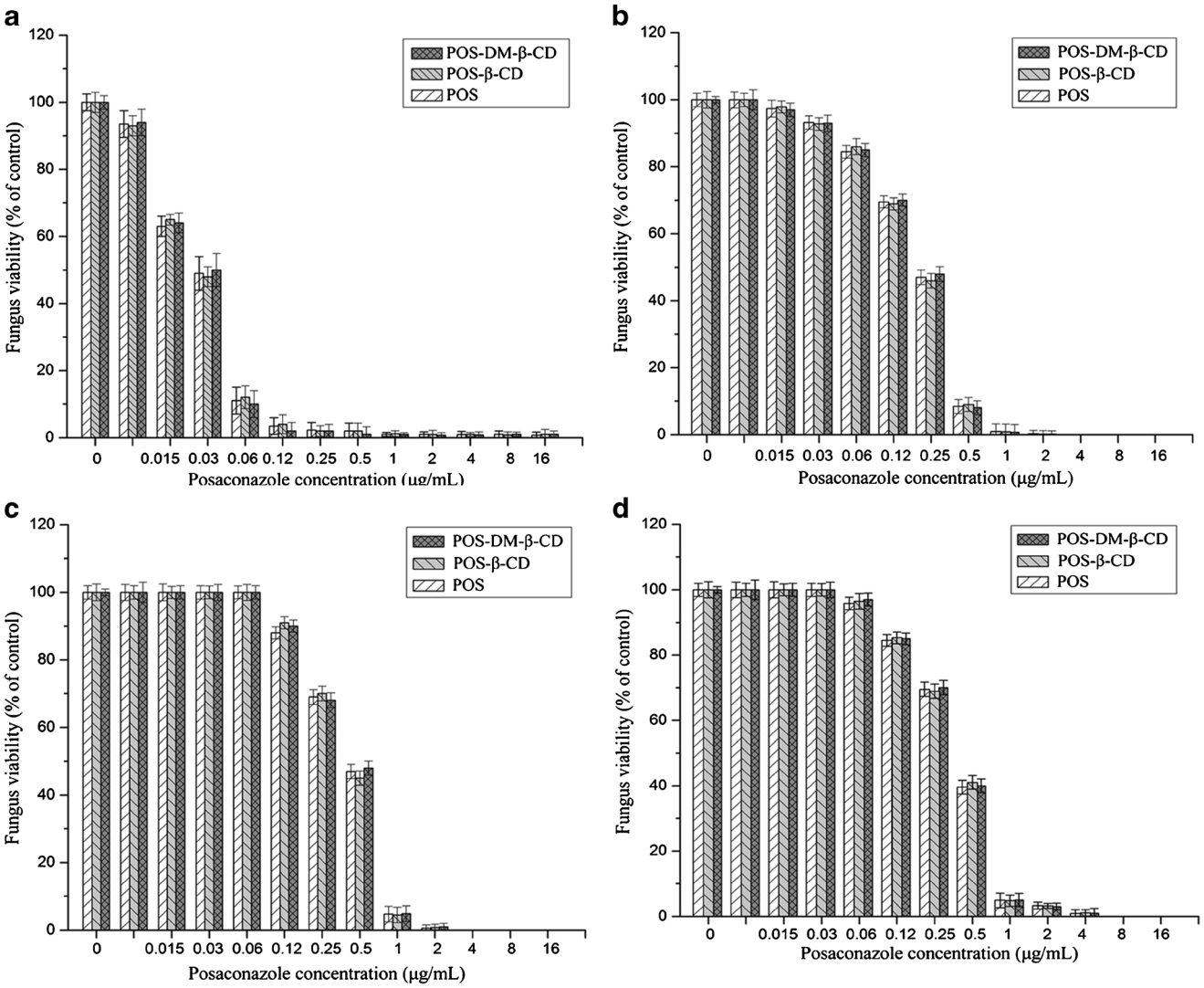

Fig. 8. *In vitro* susceptibilities of POS, β-CD–POS, and DM-β-CD–POS inclusion complex on clinical fungi isolates *Candida albicans* (**a**), *Aspergillus fumigates* (**b**), *Aspergillus niger* (**c**), and *Penicillium* spp. (**d**)

dissolved after 5 min, indicating the complexes are hopeful to be prepared as immediate release dosage form. The β-CD complex showed approximately 75% dissolution after 90 min ($P < 0.01$), whereas the DM-β-CD exhibited nearly 95% dissolution ($P < 0.001$). The enhancement of dissolution was probably due to the hydrophilic exterior surface of CDs, as the POS molecules embedded into the CD cavity to form hydrophilic complexes. The significant improvement may play key roles to improve the bioavailability of POS according to the literature (7). In addition, the DM-β-CD complex exhibits significantly better dissolution rates than the β-CD complex. These differences indicated that DM-β-CD was more capable than β-CD in forming water-soluble complexes with drugs which was predicted based on the phase solubility diagram and its higher K_s values.

These findings indicated that complexation with DM-β-CD could be a more effective strategy than β-CD to increase the dissolution rate of a poorly soluble drug.

In Vitro Antifungal Susceptibility Testing

When developing a new dosage form of a drug, maintaining high biological activity of the drug is the basis of its clinical application. Thus, evaluating the antifungal activity of POS after complexation with CD is of great significance. The results of the hole-punch method initially confirmed that the complexes retained the antifungal activity of POS (Fig. S2). Furthermore, the results of the dilution method showed the detailed antifungal properties of the inclusion complexes. The effects of free POS, β-CD–POS complex, and DM-β-CD–POS complex on the viabilities of fungi are illustrated in Fig. 8 (Fig. 8a for *C. albicans*, Fig. 8b for *A. fumigates*, Fig. 8c for *A. niger*, and Fig. 8d for *Penicillium* spp.). After incubation for 48 h, the two inclusion complexes decreased the viability of the fungi in a dose-dependent manner, which was consistent with the results of previous reports about POS antifungal activities (7–9). *C. albicans* was the most susceptible, with MIC at which 90% of the isolates were inhibited (MIC_{90}) was 0.06 μg/mL (99% of isolates were inhibited by ≤0.25 μg/mL), and *Penicillium* spp. were the least susceptible, with MIC_{90} at 1 μg/mL (95% of isolates were inhibited by ≤2 μg/mL). The inclusion complexes exhibited antifungal activities comparable with free POS ($P > 0.05$). In addition, the complexes showed better antifungal activities than itraconazole and fluconazole (37,38), which were on the market for years.

Thus, these results indicated that the two inclusion complexes exhibited vast potential for use as an antifungal agent against fungal infections.

CONCLUSIONS

In the present study, the inclusion complexes of β-CD–POS and DM-β-CD–POS with 1:2 drug–CD ratios were prepared. The high values of apparent stability constants obtained from phase solubility studies indicated that the 1:2 guest–host complexes were stable. FT-IR, PXRD, NMR, and SEM were used to characterize the solid complexes. The experimental results showed that the triazole and triazolone rings of POS were inserted into the CD cavities, which was confirmed by molecular modeling studies. After complexation with β-CD and DM-β-CD, the water solubility and dissolution rates of POS were significantly enhanced. Especially, the aqueous solubility of the DM-β-CD complex is nine times higher than that of the β-CD complex. Further *in vitro* studies showed that the two inclusion complexes retained the antifungal activities of POS. This work indicates that the DM-β-CD complex is better than β-CD complex in the preparation of novel POS solid dosage form with good water solubility, excellent dissolution, and high biological activities.

ACKNOWLEDGMENTS

This work was supported by the Applied Basic Research Project of Sichuan Province (Grant No. 2014JY0042), the Testing Platform Construction of Technology Achievement Transform of Sichuan Province (Grant No. 13CGPT0049), and the National Development and Reform Commission and Education of China (Grant No. 2014BW011). We thank the College of Polymer Science and Engineering, Sichuan University, for providing instrumentation and infrastructure for the thermal and morphology analysis.

REFERENCES

1. Keating GM. Posaconazole. Drugs. 2005;65:1553–67.
2. Sabatelli F, Patel R, Mann PA, Mendrick CA, Norris CC, Hare R, *et al. In vitro* activities of posaconazole, fluconazole, itraconazole, voriconazole, and amphotericin B against a large collection of clinically important molds and yeasts. Antimicrob Agents Ch. 2006;50:2009–15.
3. Nagappan V, Deresinski S. Reviews of anti-infective agents: posaconazole: a broad-spectrum triazole antifungal agent. Clin Infect Dis. 2007;45:1610–7.
4. Torres HA, Hachem RY, Chemaly RF, Kontoyiannis DP, Raad II. Posaconazole: a broad-spectrum triazole antifungal. Lancet Infect Dis. 2005;5:775–85.
5. Schering Corporation. Prescribing information for Noxafil (posaconazole) oral suspension. Kenilworth: Schering Corporation; 2008.
6. Europe SP. Noxafil 40 mg/ml oral suspension, summary of product characteristics. Brussels, Belgium: SP Europe; 2008.
7. Krishna G, Ma L, Vickery D, Yu X, Wu I, Power E, *et al*. Effect of varying amounts of a liquid nutritional supplement on the pharmacokinetics of posaconazole in healthy volunteers. Antimicrob Agents Ch. 2009;53:4749–52.
8. Greer ND. Posaconazole (Noxafil): a new triazole antifungal agent. Proc (Baylor Univ Med Cent). 2007;20:188–96.
9. Courtney R, Wexler D, Radwanski E, Lim J, Laughlin M. Effect of food on the relative bioavailability of two oral formulations of posaconazole in healthy adults. Brit J Clin Pharmaco. 2004;57:218–22.
10. Heimbecher SK, Monteith D, Heimbecher S, Montant D, Hembesher SK. Composition, useful to treat fungal or parasitic infections e.g. candidiasis, aspergillosis, fusariosis, scedosporiosis, Chagas disease and leishmaniasis, comprises posaconazole and modified cyclodextrin in aqueous solution, International Patent NO. WO2012005973-A1. 2012.
11. Wang D, Jiang W. Freeze-dried powder injection comprises posaconazole, cyclodextrin solubilizer and pH regulator, and prepared by adding acid to components, and using mixed solvent comprising organic solvent and water for injection, Chinese Patent NO. CN103284959-A. 2013.
12. Sathigari S, Chadha G, Phillip Lee Y-H, Wright N, Parsons DL, Rangari VK, *et al*. Physicochemical characterization of efavirenz–cyclodextrin inclusion complexes. AAPS PharmSciTech. 2009;10:81–7.
13. Ren LL, Zhou Y, Wei P, Li M, Chen GG. Preparation and pharmacokinetic study of aprepitant-sulfobutyl ether-β-cyclodextrin complex. AAPS PharmSciTech. 2014;15:121–30.

14. Tang PX, Li SS, Wang LL, Yang HQ, Yan J, Li H. Inclusion complexes of chlorzoxazone with β- and hydroxypropyl-β-cyclodextrin: characterization, dissolution, and cytotoxicity. Carbohyd Polym. 2015;131:297–305.
15. Rácz CP, Borodi G, Pop MM, Kacso L, Sánta S, Maria TC. Structure of the inclusion complex of β-cyclodextrin with lipoic acid from laboratory powder diffraction data. Acta Crystallogr B. 2012;68:164–70.
16. Saenger W. Cyclodextrin inclusion compounds in research and industry. Angew Chem Int Edit. 1980;19:344.
17. Szejtli J. Introduction and general overview of cyclodextrin chemistry. Chem Rev. 1998;98:1743–53.
18. Kratz JM, Teixeira MR, Ferronato K, Teixeira HF, Koester LS, Simoes CMO. Preparation, characterization, and *in vitro* intestinal permeability evaluation of thalidomide–hydroxypropyl-β-cyclodextrin complexes. AAPS PharmSciTech. 2012;13:118–24.
19. Huang Z, Tian SL, Ge X, Zhang J, Li SQ, Li M, *et al*. Complexation of chlorpropham with hydroxypropyl-β-cyclodextrin and its application in potato sprout inhibition. Carbohyd Polym. 2014;107:241–6.
20. Higuchi T, Connors KA. Phase solubility techniques. Adv Anal Chem Instrum. 1965;4:117–212.
21. Warren NG, Hazen KC. Candida, Cryptococcus and other yeasts of medical importance, Chaper 61. In: Murray PR, Baron ES, Pfaller MA, Tenover FC, Yolken RH, editors. Manual of Clinical Microbiology. 6th ed. Washington: ASM Press; 1995. p. 723.
22. National Committee for Clinical Laboratory Standards, Reference method for broth dilution testing of yeasts, Approved standard-second edition M27-A2, Wayne, PA: NCCLS, 2002.
23. Barry AL, Pfaller MA, Brown SD, Espinel-Ingroff A, Ghannoum MA, Knapp C, *et al*. Quality control limits for broth microdilution susceptibility tests of ten antifungal agents. J Clin Microbiol. 2000;38:3457–9.
24. Miyake K, Irie T, Arima H, Hirayama F, Uekama K, Hirano M, *et al*. Characterization of itraconazole/2-hydroxypropyl-β-cyclodextrin inclusion complex in aqueous propylene glycol solution. Int J Pharm. 1999;179:237–45.
25. Brewster ME, Vandecruys R, Peeters J, Neeskens P, Verreck G, Loftsson T. Comparative interaction of 2-hydroxypropyl-β-cyclodextrin and sulfobutylether-β-cyclodextrin with itraconazole: phase-solubility behavior and stabilization of supersaturated drug solutions. Eur J Pharm Sci. 2008;34:94–103.
26. Higuchi T, Kristiansen H. Binding specificity between small organic solutes in aqueous solution: classification of some solutes into two groups according to binding tendencies. J Pharm Sci. 1970;59:1601–8.
27. Blanco J, Vila-jato JL, Otero F, Anguiano S. Influence of method of preparation on inclusion complexes of naproxen with different cyclodextrins. Drug Dev Ind Pharm. 1991;17:943–57.
28. Pitha J, Milecki J, Fales H, Pannell L, Uekama K. Hydroxypropyl-β-cyclodextrin: preparation and characterization; effects on solubility of drugs. Int J Pharm. 1986;29:73–82.
29. Lu Y, Guo T, Qi JP, Zhang JW, Wu W. Enhanced dissolution and stability of lansoprazole by cyclodextrin inclusion complexation: preparation, characterization, and molecular modeling. AAPS PharmSciTech. 2012;13:1222–9.
30. Wang DW, Ouyang CB, Liu Q, Yuan HL, Liu XH. Inclusion of quinestrol and 2, 6-di-O-methyl-β-cyclodextrin: preparation, characterization, and inclusion mode. Carbohyd Polym. 2013;93:753–60.
31. Kfoury M, Auezova L, Fourmentin S, Greige-Gerges H. Investigation of monoterpenes complexation with hydroxypropyl-β-cyclodextrin. J Incl Phenom Macrocyle Chem. 2014;80:51–60.
32. Chen W, Yang LJ, Ma SX, Yang XD, Fen BM, Lin J. Crassicauline A/β-cyclodextrin host-guest system: preparation, characterization, inclusion mode, solubilization and stability. Carbohyd Polym. 2011;84:1321–8.
33. Onnainty R, Longhi MR, Granero GE. Complex formation of chlorhexidine gluconate with hydroxypropyl-β-cyclodextrin (HPβCD) by proton nuclear magnetic resonance spectroscopy (^{1}H NMR). Carbohyd Res. 2011;346:1037–46.
34. Yang B, Lin J, Chen Y, Liu Y, Lin J. Artemether/hydroxypropyl-beta-cyclodextrin host-guest system: characterization, phase-solubility and inclusion mode. Bioorga Med Chem. 2009;17:6311–7.
35. Duchêne D. Cyclodextrins and their industrial uses. Paris: Editions de Santé; 1987. p. 131–72.
36. de Araujo DR, Tsuneda SS, Cereda CMS, Carvalho FDGF, Preté PSC, Fernandes SA. Development and pharmacological evaluation of ropivacaine-2-hydroxypropyl-β-cyclodextrin inclusion complex. Eur J Pharm Sci. 2008;33:60–71.
37. Diekema DJ, Messer SA, Hollis RJ, Jones RN, Pfaller MA. Activities of caspofungin, itraconazole, posaconazole, ravuconazole, voriconazole, and amphotericin B against 448 recent clinical isolates of filamentous fungi. J Clin Microbiol. 2003;41:3623–6.
38. Pfaller MA, Messer SA, Hollis RJ, Jones RN. *In vitro* activities of posaconazole (Sch 56592) compared with those of itraconazole and fluconazole against 3,685 clinical isolates of Candida spp. and Cryptococcus neoformans. Antimicrob Agents Ch. 2001;45:2862–4.